Non uniqueness and uniqueness of capillary surfaces

by

Robert Finn

Max-Planck-Institut
für Mathematik
Gottfried-Claren-Straße 26
D-5300 Bonn 3

West Germany

MPI/87-36

Non uniqueness and uniqueness of capillary surfaces

Robert Finn

By *capillary surface* we mean a two dimensional surface in $\mathbb{R}^3$, whose mean curvature is a given function $\mathcal{H}(x)$, $x \in \mathbb{R}^3$, and which meets prescribed bounding walls (container) in a prescribed angle γ. For background details and derivation of the equations, see, e.g. [1]. The function $\mathcal{H}(x)$ may contain an additive constant that is not given in advance, but is to be determined by a volume constraint. Physically such surfaces are determined as equilibrium configurations for liquid-gas or liquid-liquid interfaces in solid containers, by the principle of virtual work. We restrict attention in this paper to physical surfaces in the earth's gravitational field, for which

$$\mathcal{H}(x) = \kappa z + \lambda \qquad , \quad \kappa > 0 \ , \tag{1}$$

and to surfaces in the absence of gravity, obtained by setting $\kappa = 0$ in (1).

To our knowledge, the uniqueness of such surfaces has been proved in only two cases

i) the surfaces S determined by a vertical cylindrical tube Z of general section Ω, with gravity either absent or directed downward into the fluid; surfaces satisfying the conditions do not always exist (cf [1] Chapter 6), but when they do exist they are determined either uniquely or up to vertical translation, depending on eventual volume constraint, see [1] Theorem 5.1, see also Vogel [2]

ii) a liquid drop of prescribed volume on a plane Π of homogeneous material, either in the absence of gravity or with gravity directed orthogonal to Π from the side on which the drop rests; see Wente [3] for symmetry and [1] Theorem 3.2 for the uniqueness of the symmetric surface. In this case a double infinity of equilibrium surfaces can be constructed by translation along the plane, however the surfaces are all congruent to each other, and can be considered as equivalent.

The two situations are illustrated in Figure 1. The corresponding uniqueness proofs are very different; they rely heavily on the particular geometries and do not extend to general intermediate configurations as illustrated in Figure 1. In fact, the example of Figure 2 shows that in the intermediate case uniqueness cannot always be expected. Here the container consists of a piece of right circular cone adjoined to a vertical cylinder, and is oriented to the gravity field (if there is one) as indicated.

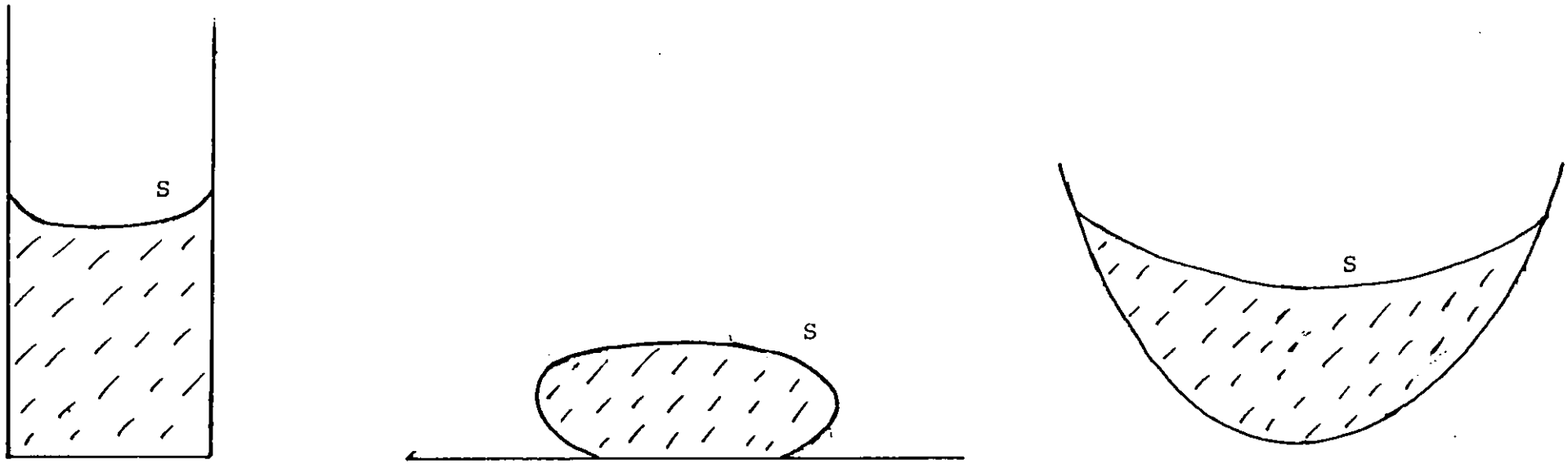

Figure 1. Cylinder plane, intermediate case

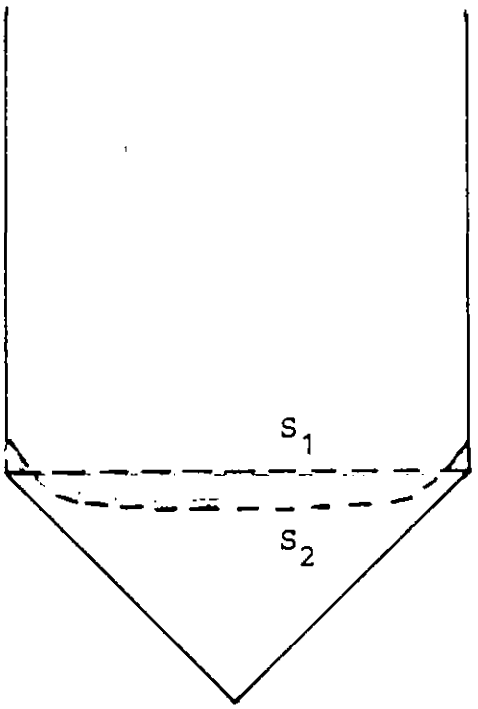

Figure 2. Nonuniqueness

If the container is filled with slightly less fluid than the volume of the cone, and if the contact angle $\gamma = \pi/4$, then one possibility is the horizontal surface S_1 indicated. However it is clear that a second surface S_2 bounding the same volume V can then be found, with contact circle on the cylinder.

For the case $\gamma = \frac{\pi}{2}$ and $g = 0$, Gulliver and Hildebrandt [4] gave a striking explicit example of a container that bounds a continuum F of (non-congruent) equilibrium surfaces, all with the same volume, and they raise the question whether containers with this property can also be found when $g \neq 0$. In § 1 we answer the question affirmatively, for any γ . In § 2 we return to the case $g = 0$ but allow general γ , and show again that containers with the desired property can be obtained.

Since according to the principle of virtual work the surfaces in F are characterized by vanishing of the first variation of mechanical energy, it follows that all surfaces in F have the same energy. It is always possible to design the container so that F contains a horizontal disk . In § 3 we examine the second variation of energy in this configuration and obtain conditions under which it can be made negative. As a consequence we are able to show that F can be embedded into a larger continuum by adjoining asymmetric surfaces, and in which all surfaces not in F have lower energy; thus it cannot be expected that the surfaces in F will be observed physically apart from exceptional circumstances. We pursue this line of reasoning further in § 4, where

we give an example of a symmetric container that differs only locally and as little as desired from a (closed) vertical circular cylinder, and which for a prescribed volume admits no symmetric surface of minimizing energy. If the cylinder deformation is removed, then the minimizer for the given volume becomes unique and symmetric.

In this connection it is worth pointing out that even for a container as simple geometrically as a closed circular cylinder, the minimizing configuration can be disconnected and in a non-trivial way nonunique. We show this by example in § 5. It seems unlikely that will happen in the case of asymmetric minimizer considered above, but we have not excluded the possibility.

Finally, in § 6 we extend the known uniqueness theorems by showing that for a symmetric container whose walls are concave to the domain (as in Figure 7), the symmetric solutions are in fact uniquely determined by the contact angle and volume.

1. Equation for the container; case $g \neq 0$. A capillary surface $u(x,y)$ subject to a volume constraint in a gravity field g directed vertically downward into the (heavier) fluid is determined by the equation

$$\text{(2)} \qquad \operatorname{div} \frac{1}{W} \nabla u = \kappa u + \lambda \ ,$$

with $W = \sqrt{1+|\nabla u|^2}$ and $\kappa > 0$ a physical constant proportional to g. Here λ is to be determined by the geometry and the constraint. The surface is to meet the container in a prescribed constant angle γ; we may assume $0 \leq \gamma \leq \pi$. In a rotationally symmetric configuration, (2) takes the form

$$(3) \qquad \frac{d}{dr}(r \sin \psi) = \kappa r u + \lambda r$$

in terms of inclination angle $\psi = \tan^{-1} u'(r)$ of the solution curve with the r-axis. In what follows, it is basic to observe that although (3) is of second order and the two integration constants together with λ lead nominally to a three parameter family of solutions, in fact *the totality of solutions of* (3) *that are defined in a deleted neighborhood of* $r = 0$ *are contained in a one parameter family of curves.*

To see that, we observe first that a vertical translation reduces any such solution to a corresponding (congruent) solution of

$$(4) \qquad \frac{d}{dr}(r \sin \varphi) = \kappa r v , \qquad \varphi = \tan^{-1} v'(r) .$$

Formal integration of (4) shows that any solution in the class considered tends to a limit $v_0 = v(0)$ as $r \longrightarrow 0$, then that $\lim_{r \to 0} v'(r) = 0$, and finally that v_0 uniquely determines the traverse. The family has the general appearance indicated in

Figure 3 . For details see [1], Chapter 2; there the following properties are established:

a) on any solution curve the values v,v' and the curvature $(\sin\varphi)_r$ increase or decrease with r, according as $v_0 > 0$ or $v_0 < 0$. Each curve becomes vertical at a value $R < \frac{2}{\kappa|v_0|}$.

b) for fixed $r = r_0$, v' increases with height z, from $-\infty$ to ∞ in a finite interval whose length decreases from ∞ to 0 as r_0 varies from 0 to ∞.

From b) we see that for any fixed r_0, the values $\sin\varphi(r_0)$ can be chosen as parameter to describe the family.

We proceed to the construction. We seek a curve $r = f(z)$, defining a container $\mathfrak{C}$, which cuts a family of solutions of (3) in constant angle γ and for which the corresponding rotation surfaces enclose with $\mathfrak{C}$ a constant volume. We set

$$(5) \qquad \xi = \frac{u'}{\sqrt{1+u'^2}} = \sin\psi\ ; \qquad \eta = \frac{r'}{\sqrt{1+r'^2}} = \cos(\psi+\gamma)$$

(see Figure 4). A given curve $f(z)$ thus determines $\xi = \xi(\eta)$ at each point on its traverse. By property b) above, the values

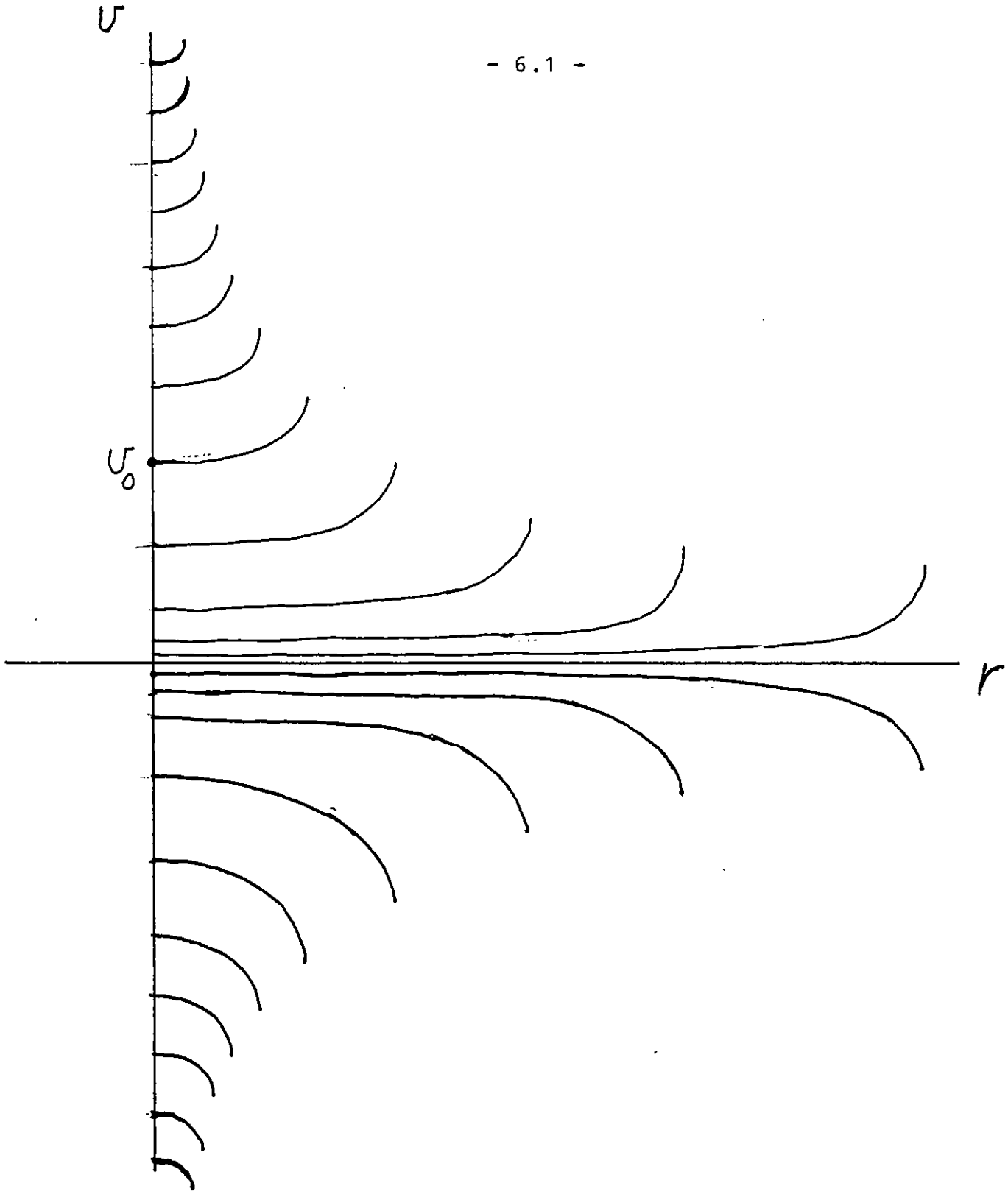

Figure 3. The disk-type solutions of (4)

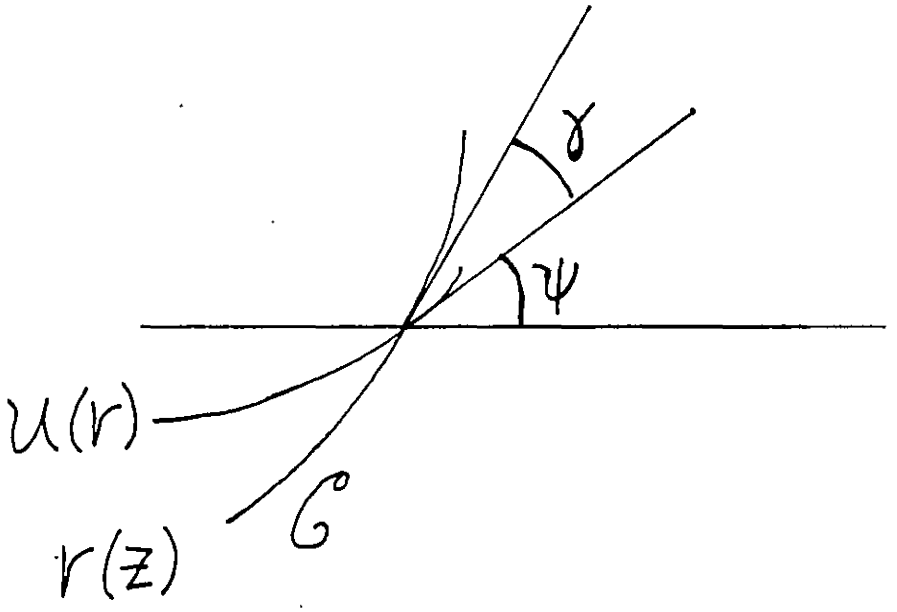

Figure 4. Intersection angles

r,ξ on the curve determine a unique solution $v(\rho;\xi(r))$, such that $\sin\varphi(r) = \xi(r)$.

Set $\delta = z - v(r;\xi(r))$. Then the condition for coincidence of the solution u of (3) with the curve $r = f(z)$ at the point (r,z) yields

$$(6) \qquad (r \sin\varphi)_r = \kappa r v(r;\xi(r)) = \kappa r(u - \delta)$$

$$= \kappa r u + \lambda r$$

with

$$(7) \qquad \lambda = -\kappa(z - v(r;\xi(r))) \ .$$

By the "basic observation" above, the sought solution $u(\rho;\xi(r))$ of (3) must be congruent to $v(\rho;\xi(r))$ under vertical translation; thus

$$(8) \qquad (\rho \sin\psi)_\rho = \kappa\rho u + \lambda\rho$$

with λ determined by (7).

Integrating (8) from 0 to r , we obtain for the (cylindrical) volume V^+ bounded between the rotation surface determined by $u(\rho;\xi(r))$ and the base plane $z = 0$

$$(9) \qquad V^{+} = \frac{2\pi}{\kappa}\,\xi r - \frac{\pi\lambda}{\kappa}\,r^{2} \quad .$$

For the corresponding volume determined by $z(r)$, we have

$$(10) \qquad V^{-} = 2\pi \int^{r} \rho z \, d\rho \quad .$$

The condition for constant enclosed volume then becomes

$$(11) \qquad (2 - \kappa r v_{\xi}) r'' - \frac{(1+r'^{2})^{3/2}}{r} \frac{\kappa r'}{r'\cos\gamma + \sin\gamma} \left\{ \frac{2}{\kappa}\,\xi - 2rv(r;\xi) - r^{2} \frac{\xi}{\sqrt{1-\xi^{2}}} \right\} - \kappa \frac{(1+r'^{2})^{3/2}}{r'\cos\gamma + \sin\gamma}\, r = 0 \; ;$$

here ξ is determined in terms of r' from (5) by

$$(12) \qquad \xi = \frac{1}{\sqrt{1+r'^{2}}} (\cos\gamma - r'\sin\gamma)$$

and $v(r;\xi)$ is the unique value at r of the solution of (4) for which $\sin\varphi(r) = \xi$. We derived (11) under the implicit assumption that the container projects simply onto the base plane, however one verifies readily that (11) holds in all cases.

We take as initial data for (11) values $\bar{r},\bar{r}'$ such that ψ as determined by (5) will lie in the range $-\frac{\pi}{2} < \psi < \frac{\pi}{2}$. Then the values of $v(r;\xi(r))$ will be smoothly determined in a

neighborhood of $(\bar{r},\bar{r}')$. The local existence of a solution of (11) thus reduces to showing that the factor $(2 - \kappa r v_\xi)$ does not vanish at $(\bar{r},\bar{r}')$. We have from (4)

$$\xi = \frac{\kappa}{r} \int_0^r \rho v(\rho;\xi(r))\,d\rho \tag{13}$$

from which

$$\begin{aligned} 1 &= \frac{\kappa}{r} \int_0^r \rho v_\xi(\rho;\xi(r))\,d\rho \\ &= \frac{1}{2}\,\kappa r v_\xi(r;\xi) - \frac{\kappa}{2r} \int_0^r \rho^2 v_{\rho\xi}(\rho;\xi(r))\,d\rho \end{aligned} \tag{14}$$

and we conclude from the above property b) that $2 - \kappa r v_\xi(r;\xi) < 0$. This completes the (local) existence proof.

2. Equation for the container; case $g = 0$. The case $\kappa = 0$ must be studied separately, as the volume is no longer determined by integration of the κu term in (3). However, the solutions through $r = 0$ are now known to be circular arcs, so that the volume can be determined geometrically. This property was exploited in [4] to obtain an example for the case $\gamma = \frac{\pi}{2}$. We extend that reasoning here to general γ .

The condition for constant volume becomes now

$$\frac{r^3}{3}\,\frac{\sin\psi\,(2+\cos\psi)}{(1+\cos\psi)^2} - \int^z r^2 dz = c\ . \tag{15}$$

We have

$$(16) \qquad \cos\psi = \cos\,(\psi+\gamma-\gamma) = \eta\cos\gamma + \sqrt{1-\eta^2}\,\sin\gamma$$

with η defined in (5). From (16) we find

$$(17) \qquad \psi'(z) = -\frac{r''}{1+r'^2}$$

and setting $w = \sqrt{1+r'^2}$ we obtain

$$(18) \qquad rr'' + w^2\cdot(2w\sin\gamma + r'\sin\gamma\cos\gamma + 1 + \sin^2\gamma) = 0 \ .$$

In the particular case $\gamma = \pi/2$, Gulliver and Hildebrandt [4] integrated (18) explicitly, obtaining

$$(19) \qquad z = \pm\sqrt{r_0^2-r^2} - \frac{r_0}{4}\ln\frac{r_0^2\pm\sqrt{r_0^2-r^2}}{r_0^2\mp\sqrt{r_0^2-r^2}} \ .$$

Also if $\gamma = 0$, (18) integrates explicitly to yield as container a continuation of the solution surface. In the general case, the integration reduces to an iteration of two first order equations, either by rewriting the equation for z in terms of r (since z does not appear explicitly) or by choosing w as independent variable. The latter choice leads to a somewhat simpler equation

$$(20) \qquad -\frac{dr}{r} = \frac{dw}{w\cdot(2w\sin\gamma+1+\sin^2\gamma+\sqrt{w^2-1}\,\cos\gamma\sin\gamma)} \ .$$

By this procedure we obtain the two explicit solutions mentioned; however the general case seems much more difficult.

We may observe that in the range $0 < \psi + \gamma < \pi$ (to which the derivation of (18) was limited) there holds $rr'' = (rr')' - r'^2 < -1 - r'^2$ by (18); we conclude easily that *the solution curve includes a loop in which* r' *varies monotonely from* $-\infty$ *to* ∞. Equation (18) was integrated numerically on a hand calculator for two values of γ. The resultant loops are compared with the explicit solution (19) in Figure 5. These loops are physically realistic only for that part of the traverse for which free surface will not cross the rigid boundary.

3. <u>The second variation</u>. The following discussion encompasses all cases considered. Capillary surfaces are characterized (cf [1], Chapter 1) as stationary (equilibrium) points for the (mechanical) energy functional. Corresponding to contact angle γ, the energy E consists of three terms:

1) *Free surface energy* E_1, proportional to the amount of surface. For a graph $u(x,y)$ over a star domain Ω, we find

$$E_1 = \sigma \int_0^{2\pi} \int_0^{\bar{r}(\theta)} \sqrt{1 + |\nabla u|^2}\, \rho d\rho d\theta \quad ; \tag{21}$$

here σ is surface tension, $\bar{r}(\theta)$ describes $\partial\Omega$.

2) *Wetting energy* E_2. For an axisymmetric container

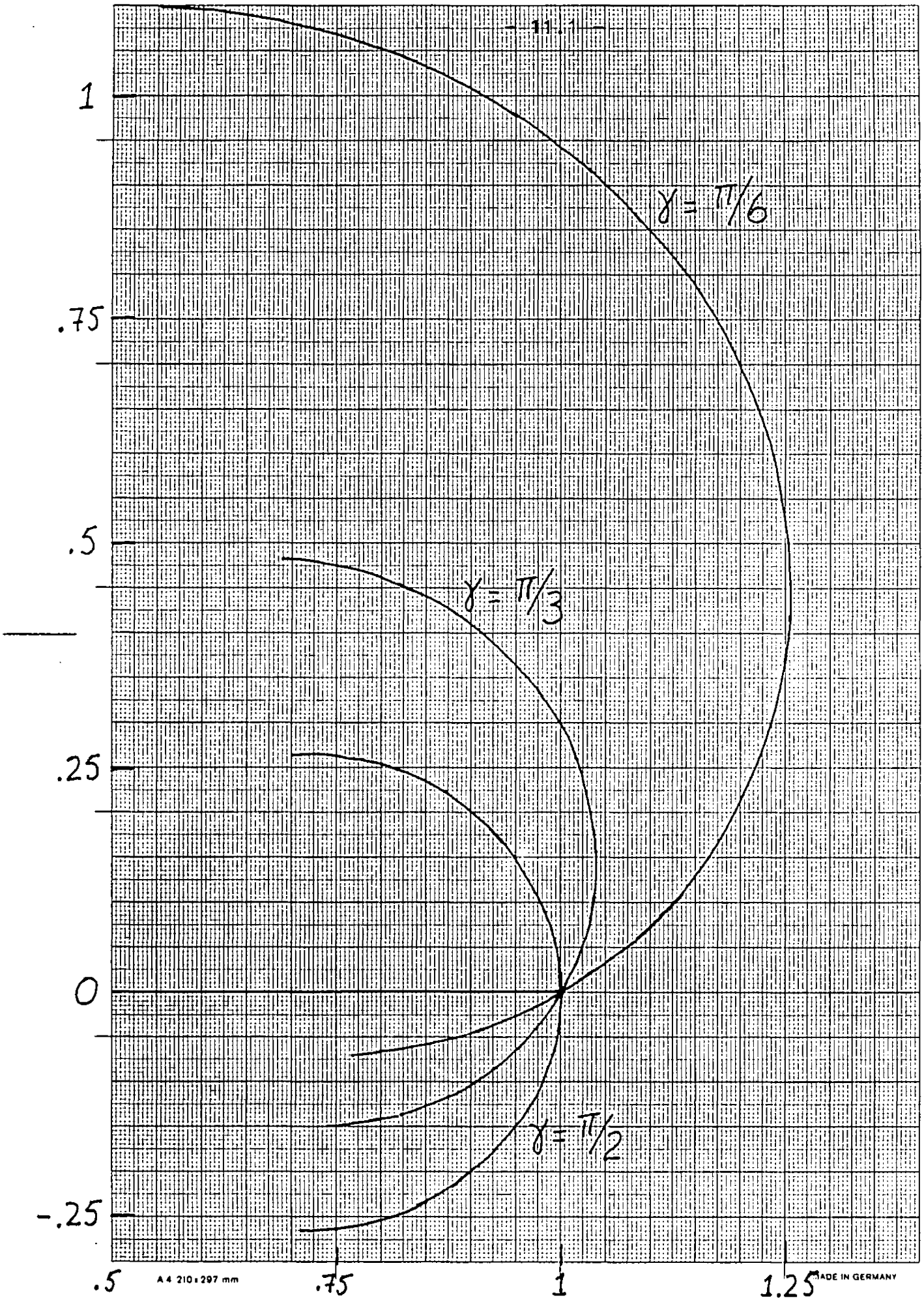

Figure 5. Exotic container profiles

$r(z)$ which intersects the surface $u(r,\theta)$ in its boundary, we have

$$(22) \qquad E_2 = -\sigma \cos\gamma \int_0^{2\pi} \int^{\bar{z}(\theta)} \sqrt{1 + r'^2}\, r dz d\theta$$

with $\bar{z}$ chosen so that $r(\bar{z}(\theta)) = \bar{r}(\theta)$.

3) *Gravitational energy* E_3 . For density difference ρ_0 (heavier fluid below) we obtain

$$(23) \qquad E_3 = \frac{1}{2} \rho_0 g \int_0^{2\pi} \int_0^{\bar{r}(\theta)} u^2 \rho d\rho d\theta \ .$$

According to the principle of virtual work, the total energy $E = E_1 + E_2 + E_3$ is stationary among all vertical perturbations (virtual displacements) $\varepsilon\zeta(\rho;\theta)$ that leave volume unchanged, i.e. for which

$$(24) \qquad \int_0^{2\pi} \int_0^{\bar{r}(\theta)} \zeta(\rho;\theta)\, \rho d\rho dv = 0 \ .$$

In what follows, we restrict attention to the particular solution $u(\rho;\theta) \equiv C$ of (2) which defines a horizontal disk $r < r_0$ in the symmetric container $r(z)$. We can arrange by vertical translation to have $C = 0$; the boundary condition then yields $r'(0) = \cot\gamma$ (see Figure 4 ,with $\psi = 0$). For the perturbation $\varepsilon\zeta(r;\theta)$ we obtain the boundary intersection curve $r = \bar{r}(\theta;\varepsilon)$,

$z = \bar{z}(\theta;\varepsilon)$ from the relation

$$z - \varepsilon\zeta(r(z);\theta) = 0 \tag{25}$$

which can be solved for $z = \bar{z}(\theta;\varepsilon)$ when ε is small enough that $1 - \varepsilon\zeta_r r' \neq 0$. We then obtain $\bar{r}(\theta;\varepsilon) = r(\bar{z}(\theta;\varepsilon))$. Differentiating (25) in ε, we find

$$\dot{\bar{z}} - \varepsilon\zeta_r r' \dot{\bar{z}} = \zeta \tag{26}$$

and since $\dot{\bar{r}} = r'\dot{z}$ we have

$$\dot{\bar{r}} = \frac{\zeta r'}{1 - \varepsilon\zeta_r r'} \ . \tag{27}$$

Using these relations, we are led to the evaluations

$$\dot{E}_1(0) = \sigma \int_0^{2\pi} \dot{\bar{r}}\,\bar{r}\,d\theta$$

$$\dot{E}_2(0) = -\sigma \int_0^{2\pi} \dot{\bar{r}}\,\bar{r}\,d\theta$$

(28 a,b,c,d)

$$\dot{E}_3(0) = 0$$

$$\dot{V}(0) = \int_0^{2\pi} \int_0^{r_0} \zeta\rho\,d\rho\,d\theta$$

$$\ddot{E}_1(0) = \sigma \int_0^{2\pi} \int_0^{r_0} |\nabla\zeta|^2 \rho d\rho d\theta + \sigma \int_0^{2\pi} (\dot{\bar{r}}^2 + \bar{r}\ddot{\bar{r}})\, d\theta$$

(29 a,b,c)

$$\ddot{E}_2(0) = -\sigma \int_0^{2\pi} (\dot{\bar{r}}^2 + \bar{r}\ddot{\bar{r}})\, d\theta + \sigma \sin^2\gamma\, \bar{r}'' \int_0^{2\pi} \zeta^2 d\theta$$

$$\ddot{E}_3(0) = \kappa\sigma \int_0^{2\pi} \int_0^{r_0} \zeta^2 d\theta$$

with $\kappa = \rho_0 g/\sigma$.

Thus for the second variation of total mechanical energy E we find

$$\frac{1}{\sigma}\ddot{E}(0) = \int_0^{2\pi} \int_0^{r_0} |\nabla\zeta|^2 \rho d\rho d\theta + \kappa \int_0^{2\pi} \int_0^{r_0} \zeta^2 \rho d\rho d\theta + \bar{r}'' r_0 \sin^2\gamma \int_0^{2\pi} \zeta^2 d\theta \quad . \tag{30}$$

We introduce the particular variation $\zeta = r\cos\theta + h(\varepsilon)$. From (25) and the boundary condition we have

$$\bar{r}(\theta) = \frac{r_0 \tan\gamma + \varepsilon h}{\tan\gamma - \varepsilon\cos\theta} + O(\varepsilon^2) \; ; \tag{31}$$

a formal calculation using (28 d) then yields $h(\varepsilon) = O(\varepsilon)$. From (30) we then find

$$\frac{1}{\pi r_0^2 \sigma}\ddot{E}(0) = 1 + \frac{1}{4}\kappa r_0^2 + \bar{r}'' r_0 \sin^2\gamma \quad . \tag{32}$$

If $\kappa = 0$ we return to (18). Since $w = \csc\gamma$ in the case

considered we obtain

$$\bar{r}'' = -\frac{4}{r_0 \sin^2 \gamma} \quad ; \tag{33}$$

thus

$$\ddot{E}(0) = -3\pi r_0^2 \sigma < 0 \tag{34}$$

and we see that *the initial surface can be embedded into a one parameter family with decreasing energy.*

If $\kappa > 0$ we find from (11), since $v \equiv 0$ and initially $\xi = 0$

$$(2 - \kappa r_0 v_\xi)\, \bar{r}'' = \frac{\kappa r_0}{\sin^2 \gamma} \quad . \tag{35}$$

In order to estimate $\bar{r}''$ we must obtain an estimate for its coefficient. From (14) we have

$$2 - \kappa r v_\xi(r;\xi(r)) = \frac{-\kappa}{r} \int_0^r \rho^2 v_{\rho\xi}(\rho;\xi(r))\, d\rho \quad . \tag{36}$$

We have already shown that $v_{\rho\zeta} > 0$. We proceed to show that it increases in ρ , on any solution curve. For fixed $r = R$, we set $\tau = \xi(R)$. Adopting τ as parameter to define the family of solutions, we have from (4)

$$\xi(r;\tau) = \frac{\kappa}{r} \int_0^r \rho v(\rho;\tau)\, d\rho \quad .$$

Thus

$$\xi_\tau(r;\tau) = \frac{\kappa}{r} \int_0^r \rho v_\tau(\rho;\tau)\, d\rho \quad . \tag{37}$$

Differentiating in r ,

$$\xi_{r\tau}(r;\tau) = -\frac{\kappa}{r^2} \int_0^r \rho v_\tau(\rho;\tau)\, d\rho + \kappa v_\tau(r;\tau)$$

and since v_τ increases in ρ ,

$$\xi_{r\tau}(r;\tau) > -\frac{\kappa}{2}\, v_\tau(r;\tau) + \kappa v_\tau(r;\tau) \tag{38}$$

$$= \frac{1}{2}\, \kappa v_\tau(r;\tau) > 0 \quad .$$

By definition

$$\xi(r;\tau) = \frac{v_r(r;\tau)}{\sqrt{1+v_r^2(r;\tau)}}$$

from which

$$\xi_\tau = \frac{1}{(1+v_r^2)^{3/2}}\, v_{r\tau}$$

$$\xi_{r\tau} = \frac{1}{(1+v_r^2)^{3/2}}\, \frac{d}{dr}\, (v_{r\tau}) - \frac{3 v_r v_{rr}}{(1+v_r^2)^{5/2}}\, v_{r\tau} > 0$$

by (38). Thus

$$(39) \qquad \frac{d}{dr} v_{r\tau} > \frac{3v_r v_{rr} v_{r\tau}}{(1+v_r^2)} > 0 \ .$$

This result holds for any $R > 0$. Setting $R = r$, τ becomes $\xi(r)$ and we obtain from (36)

$$(40) \qquad 2 - \kappa r v_\xi(r;\xi(r)) > -\kappa \frac{r^2}{3} v_{\rho\xi}(r;\xi(r)) \ .$$

Since $v_\rho = \tan\psi = \frac{\xi}{\sqrt{1-\xi^2}}$, there follows

$$2 - \kappa r_0 v_\xi(r_0;\xi(r_0)) > -\frac{\kappa r_0^2}{3\cos^3\psi}$$

and specializing to the particular solution $v \equiv 0$ we have for the coefficient in (35)

$$(41) \qquad 2 - \kappa r_0 v_\xi > -\frac{\kappa r_0^2}{3} \ .$$

We place (35) and (41) into (32) to obtain

$$(42) \qquad \ddot{E}(0) < \frac{1}{4}\kappa r_0^2 - 2$$

which is negative whenever $\kappa < 8/r_0^2$. *This condition on* κ *ensures the possibility of adjoining to the continuum* F *of symmetric solutions a family* G *of asymmetric surfaces of lower energy.*

We note that in the earth's gravitational field, $\kappa \approx 400/13$; thus the criterion is satisfied whenever $r_0 < 0{,}5$ cm . The condition is however clearly not realistic, but reflects rather a loss of information in the derivation of (41). In fact, if we parametrize the family F containing the horizontal disk by (say) the intersection height $\bar{z}$ with the container, the condition $\dot{E} \equiv 0$ in the family implies also $\ddot{E} \equiv 0$. Thus, for the particular variation, we have $\ddot{E}(0) = 0$. We denote the variation by ζ and refer to (30). We introduce a smooth $\lambda(r)$ with $|\lambda| \leq 1$ such that $\lambda \equiv 0$ in $r < r_0/3$, $\lambda \equiv 1$ in $2r_0/3 < r \leq r_0$. We find

$$\int_0^{2\pi} \zeta^2 d\theta = \int_0^{2\pi} d\theta \int_0^{r_0} (\lambda\zeta^2)_r dr$$

$$= \int_0^{2\pi} d\theta \int_0^{r_0} (\lambda_r \zeta^2 + 2\lambda\zeta\zeta_r) dr$$

$$\leq \frac{1}{|\bar{r}''| r_0 \sin^2\gamma} \int_0^{2\pi} \int_0^{r_0} |\nabla\zeta|^2 \rho d\rho d\theta + C(|\bar{r}''|+1) \int_0^{2\pi} \int_0^{r_0} \zeta^2 \rho d\rho d\theta$$

for a suitable constant C independent of the particular variation ζ. It follows that *in a sequence of configurations with* $\kappa \to \infty$, *there must hold*

$$(|\bar{r}''|+1)^2 > \kappa / C r_0 \sin^2\gamma \quad .$$

Thus we see that the restriction $\kappa < 8/r_0^2$ results apparently from inexactness in the estimates and does not seem to reflect

reality.

Finally we remark that although we have calculated the variations formally only for the circular disk, *the same considerations apply to all surfaces of* F *sufficiently close to the disk. Restricting attention to these surfaces, we see that (at least if* $\kappa < 8/r_0^2$*) none of them can be locally minimizing.*

4. Asymmetry. We construct here *an example of a symmetric container* $\mathcal{C}$ *that differs only locally and as little as desired from a circular cylinder, and which admits a family* F *with the properties* i) F *can be smoothly extended by asymmetric surfaces of lower energy as in the preceding section;* ii) *every other symmetric equilibrium surface in* $\mathcal{C}$ *yields larger energy.* In the interest of simplicity we restrict ourselves to the case $g = 0$, $\gamma = \pi/2$; the energy E then becomes, up to a multiplicative constant, the area of the free surface.

The container $\mathcal{C}$ is now determined explicitly by (19). We may take $r_0 = 1$. For $\delta > 0$ to be chosen, we consider that portion of the generating curve for which $r > 1 - \delta$, and we complete $\mathcal{C}$ with cylindrical walls as indicated in Figure 6a.

The container can be half filled on one end with liquid, leading to the family F of possible surface interfaces including the horizontal disk, as indicated in the figure. All

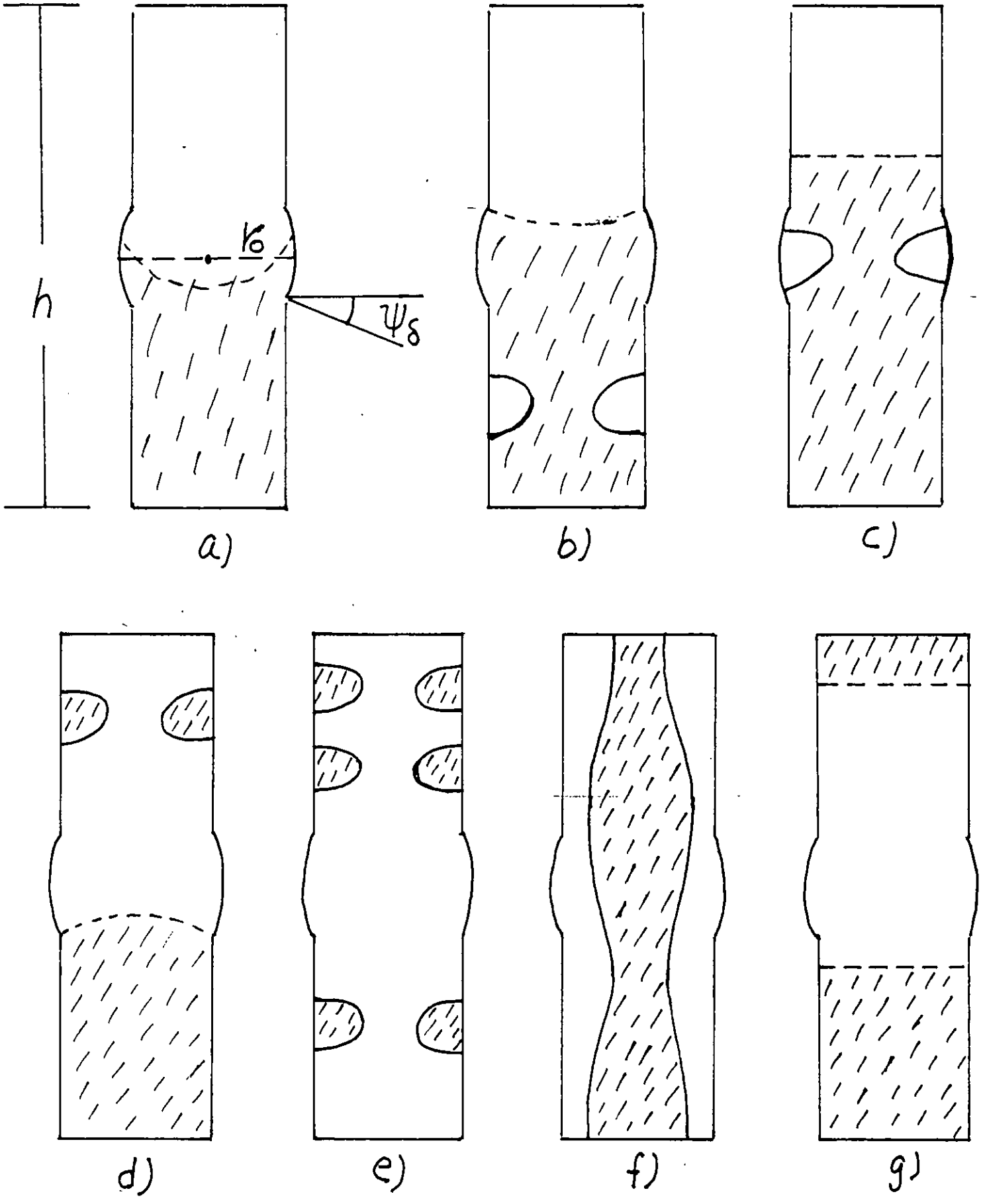

Figure 6. An exotic container; the various cases

of these configurations have equal energy E_0 , which by the result of the last section is not minimizing, even locally, if δ is small enough. We intend to show that in fact no symmetric configuration can minimize.

It is known (see remarks to follow) that every minimizing configuration is real analytic and has constant mean curvature H . The determination of the totality of symmetric surfaces in $\mathfrak{C}$ of constant H is thus reduced to quadratures, which lead to two families of surfaces, known as *unduloids* and as *nodois* (or one of their limiting configurations). These surfaces are determined by elliptic integrals; for background information, see, e.g. [5], § IV .

What are the possibilities?

a) The surface level moves up slightly as in Figure 6b, and the new volume created under the surface is filled out by an unduloid or nodoid, as in the figure. Since all bounding components of the free surface must have the same mean curvature H , the only possibility is a nodoid. Since H is the curvature of the upper spherical cap, we have $H < \sin \psi_\delta$, and thus in view of the boundary condition the inner coordinate α on the nodoid can be estimated by $\alpha < C \sin \psi_\delta$, which $\to 0$ with δ . The new surface created has area exceeding $2\pi(1 - \delta - \alpha)^2$, which together with the upper

boundary would nearly triple the original area.

A limiting case of this configuration occurs when the surface level moves further up, becoming a horizontal disk in the cylindrical part of $\mathfrak{C}$ (Figure 6c). The nodoid becomes a catenoid, which would have to lie in the deformed part of $\mathfrak{C}$, but the same reasoning applies.

b) The surface level could recede and the volume replaced by an unduloid or catenoid above, as in Figure 6d. Again the same discussion applies.

c) It could happen that no upper surface appears, and half the volume could be filled out with congruent nodoids (except for one or two exceptional ones at the ends, as in Figure 6e. In this case H (and the inner point α) need not be arbitrarily small, however there still holds $\alpha < \alpha_0 < 1$ for all possible configurations, as otherwise half the total volume could not be swept out. Thus we see that if the height h is large enough, the total free surface will again exceed the surface in F.

d) The prescribed volume could be contained in a cylinder or unduloid as in Figure 6f. Again if h is large the surface must exceed that in F. Such a configuration is in any event not stable for large h, see Athanassenas [11], Vogel [12].

e) The original column could split into two (or more) disjoint columns (Figure 6g). The total free surface would then be (essentially) at least twice that of F. We note however in this case that *by changing the relative distribution of fluid, we obtain a family of non-congruent locally minimizng configurations that cannot be deformed into a minimizing one without raising the energy.* In this connection cf the following section.

We may imagine an experiment in which $\mathfrak{C}$ is initially empty and liquid is gradually added from the bottom. Energy will remain constant until the bottom of the perturbation is reached; the energy will then increase until the contact angle $\pi/2$ is achieved with the perturbed section. At this point there is a continuous motion of the column (without increasing energy) into an asymmetric configuration with smaller energy. Although as we have seen locally stable symmetric configurations exist, it seems unlikely that they will appear, as they all have higher energy.

By a theorem of Almgren [6], see also Giusti [7], Gonzalez, Massari, Tamanini [8], Grüter [9] a minimizing configuration exists and is regular at interior points. By the above considerations it is asymmetric. It seems certain that the fluid will adopt a connected configuration without holes, but we have not proved that.

It is worth remarking that other examples of symmetric containers admitting no symmetric minimizers can be given. One possibility is a torus, in which a small drop of fluid is placed. The interest in the example we have constructed lies in the fact that it appears as an arbitrarily small deviation from a situation in which nothing exciting can occur.

5. Connectedness and disconnectedness. In the example just constructed there was heuristic reason to expect the minimizing set to be connected. We can put this reasoning into some perspective by pointing out that minimizers need not always be connected, even for containers as simple as the circular cylinder. We consider a cylinder Z of unit radius and long enough that when one fourth filled with fluid at one end, the symmetric (spherical cap) solution will cover the base, for any γ in $0 \leq \gamma \leq \pi/2$. We consider the two possibilities a) Z is half filled with fluid from one end, and b) the same volume of fluid is split into two parts, each of which covers one end. A routine calculation then yields that the energy difference $E_b - E_a < 0$ whenever

$$\cos\gamma > \frac{2}{3}\,\frac{1+\sin\gamma+\sin^2\gamma}{1+\sin\gamma} \quad . \tag{43}$$

The transition point occurs at $\gamma \approx 35.8°$.

If $\gamma = \pi/2$ the single component is preferred, supporting the conclusions of § 4.

In the above example the spherical cap is uniquely determined as the only stationary surface covering (not necessarily simply) the base, see Vogel [2]. Asymmetric solutions (minimizing or not) cannot appear.

6. Uniqueness. We return now to the original question raised in the Introduction, as to what support surfaces $\mathcal{C}$ (intermediate between plane and cylinder) will lead to unique determination of a capillary surface, for prescribed volume and contact angle. In view of the examples in [4] and in § 1 of this paper, it must be expected that the formulation of precise general conditions will not be easy. We assert, however, that *for a symmetric* $\mathcal{C}$ *concave to the domain of the fluid* (Figure 7) *and nondecreasing in height with* r , *the symmetric solution is uniquely determined.* Here the concavity need not be strict. In the assertion we assume either $g = 0$ or gravity directed downward toward $\mathcal{C}$. If $g = 0$ the solution surfaces are spherical caps and the proof reduces to an exercise that we leave to the reader. In what follows we assume that the surfaces are determined by (3) with $\kappa > 0$.

We reduce the proof of the assertion to the result of § 4.1 in [10], which can be paraphrased as follows: *The volume* $V(r_0)$

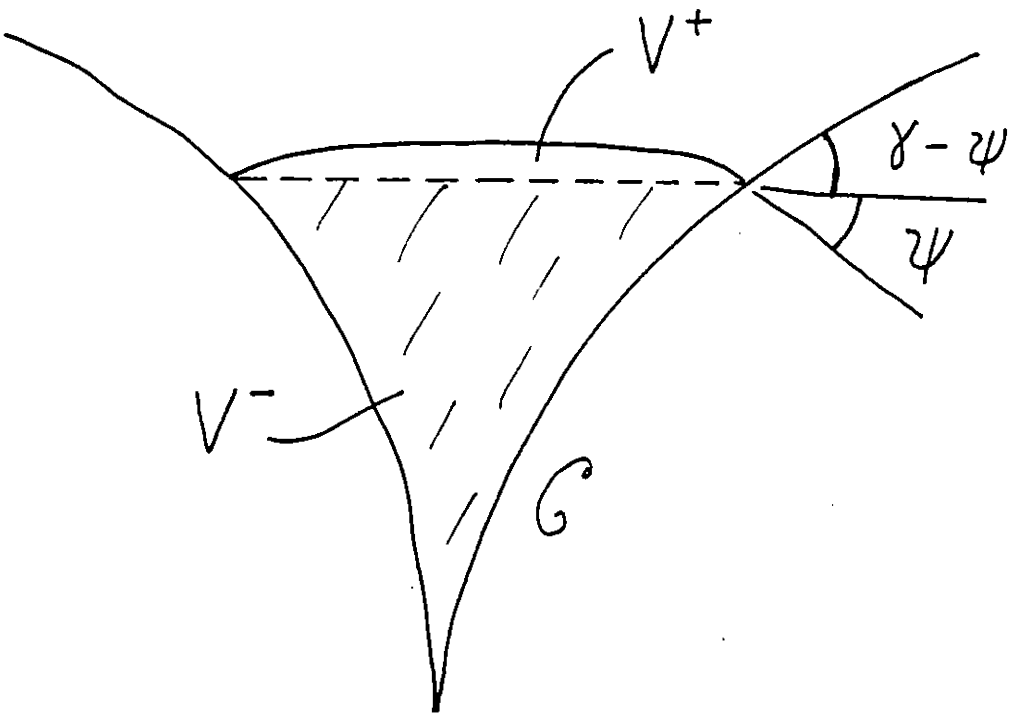

Figure 7. Container that yields uniqueness

of the (unique) sessile drop, symmetric with respect to the axis $r = 0$ *, resting on a horizontal plane* Π *and meeting* Π *in the angle* γ *at* $r = r_0$ *with* $0 < \gamma \leq \pi$ *, increases strictly in* r_0 .

We first extend the theorem as follows:

Lemma: *Let* $\psi(r)$ *be nondecreasing in* $r, 0 < \psi \leq \pi$. *Then the theorem holds with* γ *replaced by* $\psi(r)$.

To prove the lemma, we choose a fixed $r = \bar{r}$, and let $\bar{V}(r)$ be the volume of the drops with fixed angle $\gamma = \psi(\bar{r})$. Then $\bar{V}(\bar{r}) = V(\bar{r})$ and $\frac{d}{dr}\bar{V}(r) > 0$ by the theorem. We consider first the case $\psi(\bar{r}) < \pi/2$ and introduce a value $r = \bar{r} + \varepsilon$, ε small positive. The drop profiles through r corresponding to $\psi(r)$ and to $\gamma = \psi(\bar{r})$ are determined according to the "basic observation" of § 1. We need only move upward in Figure 3 on a vertical line through r , observing that ψ increases monotonely from 0 to $\pi/2$. Thus there are unique points $\bar{v}(r)$ and $v(r)$ at which γ and $\psi(r)$ are achieved, with $v \geq \bar{v}$. Now note that $\psi(r) \geq \bar{\psi}(r)$ on the entire solution trajectories through (r,v) and $(r,\bar{v})$. Therefore if we lower the upper trajectory by translation a distance δ until the end points coincide, we obtain $v - \delta \leq \bar{v}$ on the interval $0 \leq \rho \leq r$, and we conclude that for the associated sessile drops there holds $V \geq \bar{V}$. Letting $r \searrow \bar{r}$, we conclude

$\frac{dV}{dr} \geq \frac{d\bar{V}}{dr}$ and thus $\frac{dV}{dr} > 0$. Since $\bar{r}$ is arbitrary, this holds for all r at which $\psi(r) < \pi/2$.

It remains to discuss the case $\psi(\bar{r}) \geq \pi/2$. Here we use the general properties, proved in [10 § 4.1] that the curves in Figure 3 can be continued till $\psi = \pi$, and that for any fixed ψ in $0 < \psi \leq \pi$ there holds

$$(44) \qquad \frac{\partial r}{\partial v_0} < 0 \quad , \qquad \frac{\partial V}{\partial v_0} < 0$$

for the function $r(\psi;v_0)$, $V(\psi;v_0)$ arising from the solution. From the relation

$$r(\psi;v_0) = \bar{r}$$

we conclude

$$\left.\frac{\partial r}{\partial \psi}\right]_{v_0} \left.\frac{\partial \psi}{\partial v_0}\right]_{\bar{r}} + \left.\frac{\partial r}{\partial v_0}\right]_{\psi} = 0$$

when $\psi > \pi/2$ and thus $\left.\frac{\partial \psi}{\partial v_0}\right]_{\bar{r}} < 0$. Thus in order to increase ψ from $\gamma = \bar{\psi}(r)$ to the given $\psi(r)$ it is necessary to decrease v_0 (see Figure 8). The corresponding volume $V(\psi;v_0)$ exceeds $V(\gamma;v_0)$ which by (44) exceeds the original $\bar{V}$. This completes the proof of the lemma.

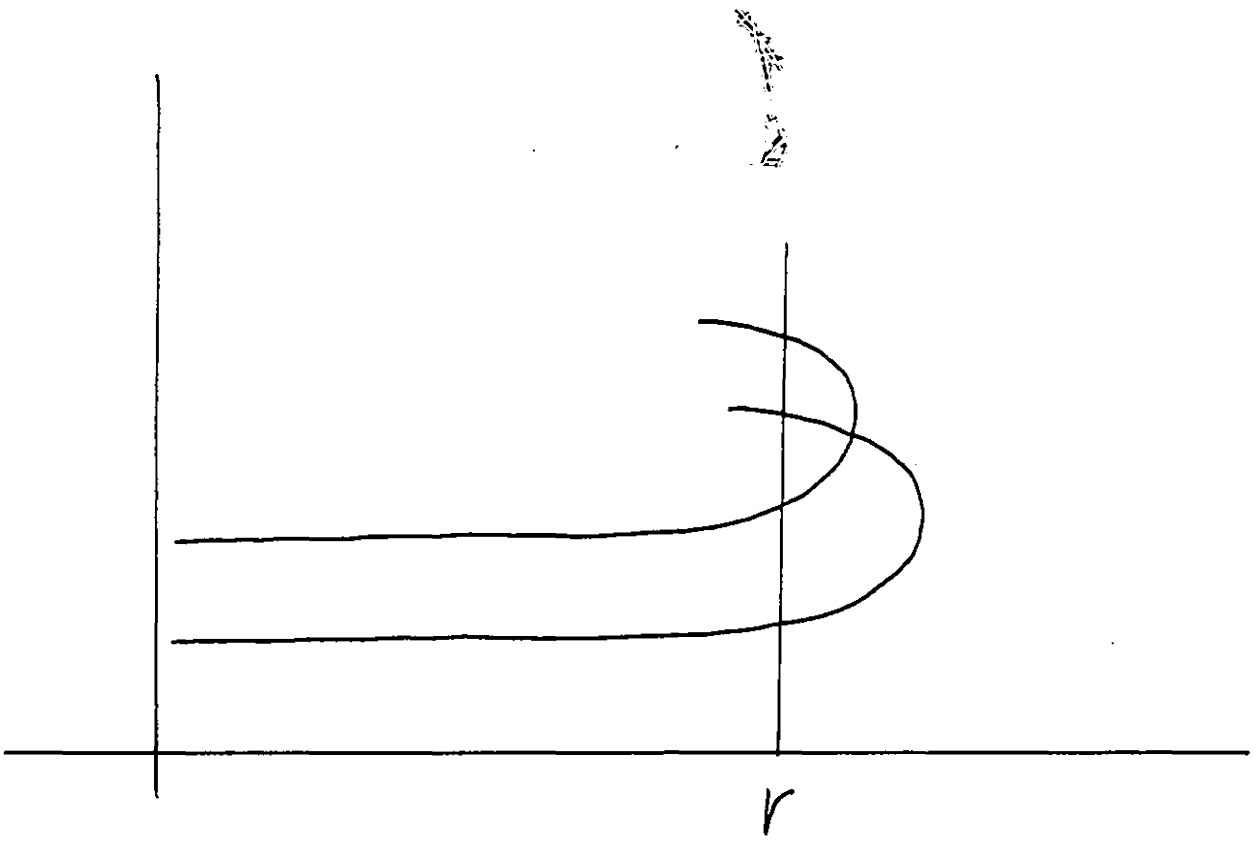

Figure 8. Uniqueness proof; case $\psi(\bar{r}) \geq \pi/2$